Engineering Journal of University of Qatar , Vol. 10, 1997, p. 123 - 132

ANALYSIS OF THE COUPLING GAP BETWEEN MICROSTRIP ANTENNAS

Moataza A. Hindy and Abdela Aziz A. Mitkees
Electrical Engineering Department, University of Bahrain
Isa Town, State of Bahrain.

ABSTRACT

The accurate and efficient Galerkin's method was developed in the spectral domain for analyzing gap discontinuities in patch antenna array. Using new current distribution the problem is solved using full wave approach rather than quasi-static approximation. The new current distribution speeds up the convergence of the solution for obtaining the resonance frequency of the system with electric and magnetic walls at the planes of symmetry. The equivalent circuit of the gap is determined for different gap sizes.

Keywords: Microstrip, Patch antenna, Coupled arrays, Microstrip resonator, Coupling gap.

INTRODUCTION

One of the effective methods for increasing the bandwidth of patch antenna is to add two resonators which are coupled to the patch radiating edges [1]. The coupling gap between the two opened rectangular patches were modeled as two dimensional capacitive networks as shown in Fig. 1. The values of these capacitance's are obtained using formulas given in reference [2] for even and odd modes of coupled microstrips of unequal widths. Complete characterization of the gap is presented in this paper. Galerkin's technique is applied in the spectral domain to solve the microstrip resonators problem. The characteristic equations for resonant frequencies are derived for both electric and magnetic walls at the planes of structure symmetry. The new current distribution basis functions which are transformed into Bessel functions in the spectral domain, reduces computational time with good accuracy.

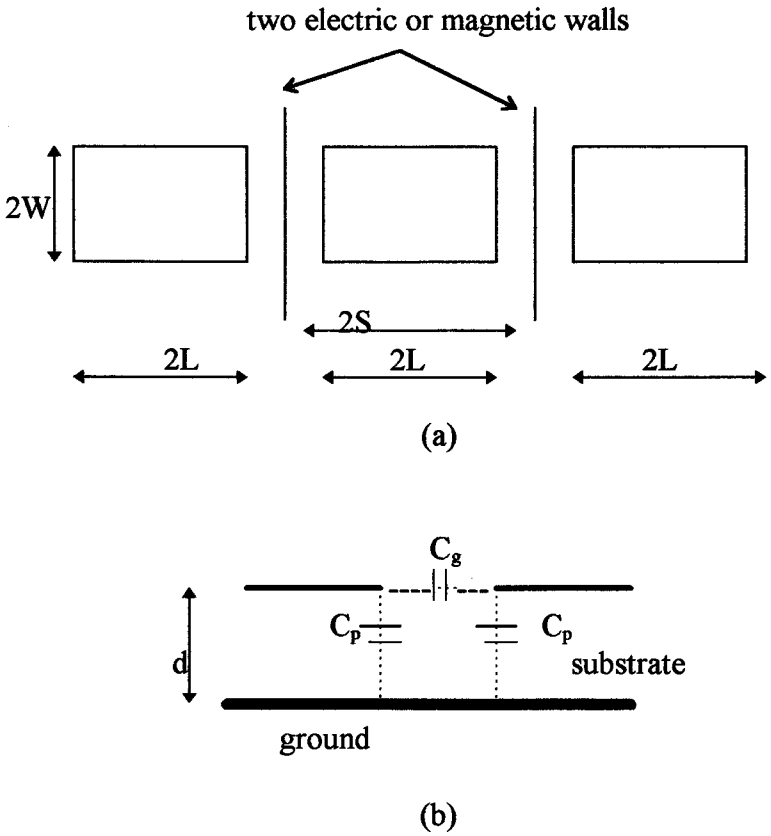

Fig. 1. Patch array: (a) Gap coupled resonators, (b) Gap equivalent circuit

ANALYSIS OF MICROSTRIP RESONATOR

The fields existing in the structure are obtained from the superposition of TE and TM fields. They can be expressed in terms of two scalar potentials e(x, y, z) and h(x, y, z) as follows:

$$E_{zi}(x,y,z) = k_1^2 e_i + \partial^2 e_i / \partial z^2 \quad (1\text{-a})$$

$$H_{zi}(x,y,z) = k_1^2 h_i + \partial^2 h_i / \partial z^2 \quad (1\text{-b})$$

$$E_{xi}(x,y,z) = \partial^2 e_i / \partial x \partial z - j\omega\mu_i(\partial h_i / \partial y) \quad (1\text{-c})$$

$$H_{xi}(x,y,z) = \partial^2 h_i / \partial x \partial z + j\omega \in_i (\partial e_i / \partial y) \quad (1\text{-d})$$

where i = 1 or 2 ,designates the substrate or air region.

$$\in_1 = \in_0 \in_r, \in_2 = \in_0, \mu_1 = \mu_0\mu_r, \mu_2 = \mu_0$$

The field components are transformed into the spectral domain using Fourier transforms

$$\tilde{e}_i(\alpha,y,\beta) = \int_{-\infty}^{\infty} dz \int_{-\infty}^{\infty} dx\, e_i(x,y,z)\exp(j\alpha x)\exp(j\beta z) \quad (2\text{-a})$$

$$\tilde{h}_i(\alpha,y,\beta) = \int_{-\infty}^{\infty} dz \int_{-\infty}^{\infty} dx\, h_i(x,y,z)\exp(j\alpha x)\exp(j\beta z) \quad (2\text{-b})$$

where α and β are Fourier transform variables. The boundary conditions [3] are transformed and applied to the Fourier transforms of the field equations (1-a) to (1-d) to obtain the solutions of field components in Fourier domain as follows:

$$\tilde{e}_1(\alpha,y,\beta) = A(\alpha,\beta)\mathrm{Sinh}(\gamma_1 y) \quad (3\text{-a})$$

$$\tilde{h}_1(\alpha,y,\beta) = B(\alpha,\beta)\mathrm{Cosh}(\gamma_1 y) \quad (3\text{-b})$$

$$\tilde{e}_2(\alpha,y,\beta) = C(\alpha,\beta)\ \exp\left[-\gamma_2(y-d)\right] \quad (3\text{-c})$$

$$\tilde{h}_2(\alpha,y,\beta) = D(\alpha,\beta)\ \exp\left[-\gamma_2(y-d)\right] \quad (3\text{-d})$$

A, B, C, D are unknowns which are obtained from applying the continuity conditions at the interface y = d in the spectral domain [3]. The coefficients are expressed in terms of the unknown strip currents $J_x(x, z)$ and $J_z(x, z)$.
The final boundary condition is:

$$E_x(x,d,z) = E_z(x,d,z) = 0 \qquad |x| < W, |z| < L \quad (4)$$

while E_x (x, d, z) and E_z (x, d, z) have different values in the dielectric regions.

This condition is applied in the spectral domain to eliminate the unknown coefficients and obtain the following coupled equations:

$$\tilde{E}_x(\alpha,\beta) = U_1(\alpha,\beta)\tilde{J}_x(\alpha,\beta) + U_2(\alpha,\beta)\tilde{J}z(\alpha,\beta) \quad (5\text{-a})$$

$$\tilde{E}_z(\alpha,\beta) = U_3(\alpha,\beta)\tilde{J}_x(\alpha,\beta) + U_4(\alpha,\beta)\tilde{J}z(\alpha,\beta) \quad (5\text{-b})$$

where U_1, U_2, U_3 and U_4 are the Fourier transform of the Green's functions, $\tilde{J}_x$ and $\tilde{J}_z$ are the Fourier transforms of the unknown patch currents.

CURRENT DISTRIBUTION FUNCTIONS

Accurate knowledge of x and z components of patch current distributions helps in accurate evaluation of patch dispersion characteristics. The choice of the basis functions is very important in problem convergence and computational time. In this work a new current distribution function is assumed in the form:

$$J_x(x,z) = \sum_{n=0}^{\infty} A_n X_n(x,z) \quad (6\text{-a})$$

$$J_z(x,z) = \sum_{n=0}^{\infty} B_n Z_n(x,z) \quad (6\text{-b})$$

Where A_n and B_n are unknown coefficients to be solved and the basis X_n and Z_n has the forms:

$$X_n(x,z) = \frac{-jSin(n+1)Q}{(n+1)\pi W} \cdot \frac{-jSin(n\bar{Q})}{\left(L^2 - z^2\right)^{\frac{1}{2}}} \quad (7\text{-a})$$

$$Z_n(x,z) = \frac{Cos(nQ)}{\left(W^2 - x^2\right)^{\frac{1}{2}}} \cdot \frac{Cos(n+1)\bar{Q}}{(n+1)\pi L} \quad (7\text{-b})$$

where $Q = Sin^{-1}(x/W)$, $\bar{Q} = Sin^{-1}(z/L)$

The Fourier transforms of (6) are given by:

$$\tilde{J}_x(\alpha,\beta) = \sum_{n=0}^{\infty} A_n \frac{J_{n+1}(\alpha W)}{\alpha W}.J_n(\beta L) \qquad (n \text{ odd}) \tag{8-a}$$

$$\tilde{J}_z(\alpha,\beta) = \sum_{n=0}^{\infty} B_n J_n(\alpha W).\frac{J_{n+1}(\beta L)}{\beta L} \qquad (n \text{ even}) \tag{8-b}$$

where $J_n(\alpha W)$ and $J_n(\beta L)$ are Bessel functions.

PATCH RESONANCE FREQUENCY

Substituting equation(8) into equation (5) and taking the inner products with the basis functions X_i and Z_i for different values of i, one applies Parseval's relations to obtain the matrix equations:

$$\sum_{m=0}^{\infty} A_m F_{im} + \sum_{n=0}^{\infty} B_n G_{in} = 0 \qquad (m,i \text{ odd}),(n \text{ even}) \tag{9-a}$$

$$\sum_{m=0}^{\infty} A_m H_{im} + \sum_{n=0}^{\infty} B_n K_{in} = 0 \qquad (n,i \text{ even}),(m \text{ odd}) \tag{9-b}$$

where

$$F_{im} = \int_{-\infty}^{\infty}\int_{-\infty}^{\infty} U_1 \frac{J_{m+1}(\alpha w)}{\alpha W} J_m(\beta L).\tilde{X}_i(\alpha,\beta)\,d\alpha\,d\beta \tag{10-a}$$

$$G_{in} = \int_{-\infty}^{\infty}\int_{-\infty}^{\infty} U_2 \frac{J_{n+1}(\beta L)}{\beta L} J_n(\alpha\beta).\tilde{X}_i(\alpha,\beta)\,d\alpha\,d\beta \tag{10-b}$$

$$H_{im} = \int_{-\infty}^{\infty}\int_{-\infty}^{\infty} U_3 \frac{J_{m+1}(\alpha W)}{\alpha W} J_m(\beta L).\tilde{Z}_i(\alpha,\beta)\,d\alpha\,d\beta \tag{10-c}$$

$$K_{in} = \int_{-\infty}^{\infty}\int_{-\infty}^{\infty} U_2 \frac{J_{n+1}(\beta L)}{\beta L} J_n(\alpha W).\tilde{Z}_i(\alpha,\beta)\,d\alpha\,d\beta \tag{10-d}$$

The determinant of the coefficient matrix must be equal to zero for a certain value of complex frequency f. the values of m, n and i must be truncated.

ANALYSIS OF THE GAP IN PATCH ARRAY

Gap parameters are obtained using the same analysis of the patch with additional two electric and magnetic walls placed at the planes of symmetry as shown in Fig.1. When walls are used the modes in the x-direction will be discrete rather than continuous modes existing in open structures. So the transformation in x-direction will be discrete Fourier variable η_k depending on the kind of walls as follows [3]:

For electric walls

$$\eta_k = (k-1/2)\pi/s \qquad \text{for } E_z \text{ even} - H_z \text{ odd(in x) modes} \tag{11-a}$$

$$\eta_k = k\pi/s \qquad \text{for } E_z \text{ odd} - H_z \text{ even(in x) modes} \tag{11-b}$$

For magnetic walls

$$\eta_k = k\pi/s \qquad \text{for } E_z \text{ even} - H_z \text{ odd(in x)} \tag{11-c}$$

$$\eta_k = (k-1/2)\pi/s \qquad \text{for } E_z \text{ odd} - H_z \text{ even(in x)} \tag{11-d}$$

where k = 1, 2, 3, ...

The new resonance frequency corresponding to electric wall structure is f_e and that for magnetic wall is f_m. The corresponding wave lengths are:

$$\lambda e = C / f_e(\epsilon_{re})^{1/2} \tag{12-a}$$

$$\lambda m = C / f_m(\epsilon_{re})^{1/2} \tag{12-b}$$

where C is the free space velocity of light, ϵ_{re} is the effective dielectric constant given in reference [4] for dispersive behavior of microstrips.

EQUIVALENT CIRCUIT OF THE GAP

Open-ended gap in microstrip patches are represented by an extension in the patch length Δl_e for electric walls and $\Delta 1_m$ for magnetic walls where:

$$\Delta l_e = (\lambda_e / 2 - 2L) / 2 \quad (13\text{-a})$$

$$\Delta l_m = (\lambda_m / 2 - 2L) / 2 \quad (13\text{-b})$$

The equivalent capacitance's [5] are given by:

$$C_e = \Delta l_e (\epsilon_{re})^{1/2} / C\, Z_0 \quad (14\text{-a})$$

$$C_m = \Delta l_m (\epsilon_{re})^{1/2} / C\, Z_0 \quad (14\text{-b})$$

where Z_0 is the characteristic impedance[4], [6] C_e and C_m are related to the π-circuit of the gap by the equations:

$$C_g = (C_e - C_m) / 2 \quad (15\text{-a})$$

$$C_p = C_m \quad (15\text{-b})$$

NUMERICAL RESULTS AND CONCLUSION

The complex resonance frequencies at both electric and magnetic walls are computed to evaluate the equivalent π-network of the coupling gap. The imaginary part of the frequency represents the radiation losses from the fringing fields at the patch ends. The series capacitance C_g (Fig. 2) increases as the gap decreases which agree with the capacitor basic idea. Capacitance C_p is negative because the gap reduces the overall microstrip shunt capacitance in the vicinity of the symmetrical plane. The new current distribution reduces the computational time due to the fast problem convergence. The matrix size is increased to (6x6) to obtain satisfactory results, truncation error is less than 5% compared to experimental work in reference [1] . The method is effective in solving antenna arrays and other complicated structures. Tables 1 and 2 show some results for different Teflon substrates with dielectric constant ϵ_r = 2.2 and d = 0. 17 cm and substrates having ϵ_r = 2.55 and d = 0. 159 cm.

Table 1. Gap Parameters for $\epsilon_r = 2.2$, d = 0. 17 cm, 2W = 3.95 cm.

2L = 0.52 cm		
Spacing (2S) cm	0.15	0.19
f_e GHz	$3.731 + j\,0.75 \times 10^{-4}$	$2.877 + j\,0.24 \times 10^{-6}$
f_m GHz	$5.235 + j\,0.125 \times 10^{-6}$	$5.257 + j\,0.177 \times 10^{-5}$
2L = 2.71		
Spacing cm	0.15	0.19
f_e GHz	$3.722 + j\,0.118 \times 10^{-3}$	$3.599 + j\,0.559 \times 10^{-6}$
f_m GHz	$5.201 + J\,0.611 \times 10^{-5}$	$5.242 + J\,0.539 \times 10^{-8}$

Table 2. Gap Parameters $\epsilon_r = 2.55$, d = 0.159 cm, 2W = 3.95 cm, 2L = 2.71 cm

Spacing (cm)	0.15	0.17	0.19	0.2
f_{re} GHz	$4.797 - j\,0.24 \times 10^{-6}$	$4.799 - j\,0.29 \times 10^{-6}$	$4.841 - j\,0.901 \times 10^{-6}$	$4.849 - j\,0.409 \times 10^{-6}$
f_{rm} GHz	$5.001 - j\,0.909 \times 10^{-8}$	$4.99 - j\,0.158 \times 10^{-7}$	$4.98 - j\,0.232 \times 10^{-7}$	$4.899 - j\,0.281 \times 10^{-7}$
C_g (Pf)	0.0885	0.0843	0.0802	0.07151
C_p (Pf)	-2.2895	-2.2831	-2.2764	-2.2822

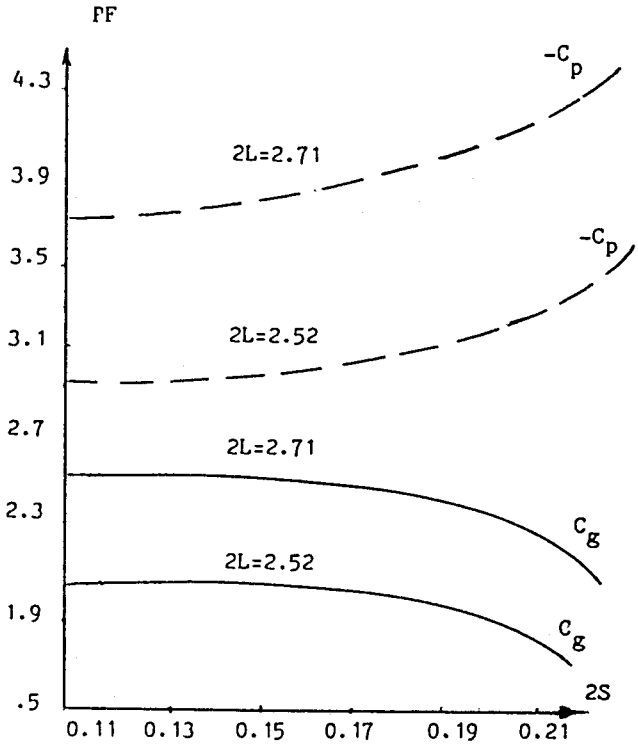

Fig. 2. C_g and $-C_p$ versus spacing for different patch lengths

REFERENCES

1. **Kumar and Gupta, 1984.** Broad Band Microstrip Antennas Using Additional Resonators Gap-Coupled to the Radiating Edges, IEEE Trans. AP, 32, No. 12 , pp.1375-1379.

2. **Garg, 1979.** Design Equation for Coupled Micorstrip Lines, Int. J. Electron, 47, pp. 587-591.

3. **Itoh. T., 1974.** Analysis of micro strip resonators, IEEE Trans. MTT, Vol. 22, pp. 946-952.

4. **Garg, 1979.** A microstrip design guide. Int. J. Electron., Vol. 46, pp. 187-192.